INSTITUTE OF PHYSICS PUBLISHING JOURNAL OF PHYSICS: CONDENSED MATTER

J. Phys.: Condens. Matter **16** (2004) S5607–S5614 PII: S0953-8984(04)79310-8

# Residual resistivity of diluted III–V magnetic semiconductors

**I Turek[1,2,3], J Kudrnovský[3,4], V Drchal[3,4] and P Weinberger[3]**

[1] Institute of Physics of Materials, Academy of Sciences of the Czech Republic, Žižkova 22, CZ-61662 Brno, Czech Republic
[2] Department of Electronic Structures, Charles University in Prague, Ke Karlovu 5, CZ-12116 Prague 2, Czech Republic
[3] Centre for Computational Materials Science, Technical University of Vienna, Getreidemarkt 9, A-1060 Vienna, Austria
[4] Institute of Physics, Academy of Sciences of the Czech Republic, Na Slovance 2, CZ-18221 Prague 8, Czech Republic

E-mail: turek@ipm.cz

Received 15 April 2004
Published 19 November 2004
Online at stacks.iop.org/JPhysCM/16/S5607
doi:10.1088/0953-8984/16/48/017

**Abstract**

The electronic structure and residual resistivity of diluted (Ga, Mn)As magnetic semiconductors are calculated from first principles using the linear muffin-tin orbital method, the coherent potential approximation, and the Kubo–Greenwood linear response theory. Particular attention is paid to the role of native compensating defects such as As antisites and Mn interstitials as well as to different magnetic configurations of the local Mn moments. The order of magnitude of the calculated resistivities compares reasonably well with available experimental data. The concentration variations of the resistivity reflect two basic mechanisms, namely the strength of the impurity scattering and the number of carriers. In agreement with a recent experiment, the calculated resistivities are strongly correlated with the alloy Curie temperatures evaluated in terms of a classical Heisenberg Hamiltonian.

## 1. Introduction

The p-type diluted magnetic semiconductors (DMSs) have recently attracted interest because of the appearance of a ferromagnetic order of the impurity local magnetic moments mediated by holes in the valence band of the parent semiconductor [1–3]. Applications in spintronics require DMSs with Curie temperatures above room temperature, which has stimulated a lot of research effort focused on the origin of the ferromagnetic exchange interactions and on the role of structural defects in these materials [4, 5]. The III–V DMSs, such as Mn doped GaAs, GaN, and InAs with Mn atoms substituting for the cations, represent the most frequently studied

  

systems of this class [1]; existing theoretical studies include first-principles calculations of the exchange interactions and the Curie temperatures [6–9]. The theoretical studies of transport properties of these systems, on the other hand, remain confined to a model level [10, 11]. It has been shown in a recent experiment [12] that controlled annealing of thin (Ga, Mn)As films accompanied by monitoring of the resistivity during growth can lead to high Curie temperatures of the films. Moreover, a pronounced correlation between the Curie temperatures and the conductivities of the real samples has been reported [12].

Motivated by these findings, we present here results of systematic first-principles calculations of the residual resistivity of (Ga, Mn)As alloys. Particular attention is paid to the influence of various kinds of compensating defects on this basic zero-temperature transport property that reflects processes of electron scattering on randomly placed impurities. Besides looking at the effect of As antisite atoms (As atoms occupying the cation sublattice) [4], we have investigated the effect of Mn interstitials (Mn atoms occupying the interstitial positions of the zinc-blende structure) [13]; both defects act as double donors, thus reducing the number of the valence holes considerably. Since recent theoretical studies indicate that magnetic structures with partial disorder of local Mn magnetic moments can lower the total energy of the system as compared to that for the ferromagnetic state [5], we have included the magnetic disorder in our models. Similarly, we have calculated the resistivity for different orientations of the Mn magnetic moments on the substitutional and interstitial positions. Finally, we estimate the alloy Curie temperatures and present their correlation with the calculated conductivities.

## 2. Models, formalism, and numerical details

The systems studied were derived from Mn doped GaAs (zinc-blende structure) with a fixed lattice constant equal to that of pure GaAs ($a = 0.5653$ nm). The alloys without structural defects are described as $(Ga_{1-x}Mn_x)As$, where $x$ denotes the concentration of Mn atoms substituting randomly for Ga atoms on the cation sublattice. Alloys with As antisites are simulated as $(Ga_{1-x-y}Mn_xAs_y)As$, where $y$ denotes the As antisite content. For inclusion of the magnetic disorder, pseudoquaternary alloys on the cation sublattice were introduced with a formula $(Ga_{1-x-y}Mn^{+}_{x-c}Mn^{-}_{c}As_y)As$, where $c$ is an auxiliary concentration variable ($0 \leqslant c \leqslant x$) which specifies the content of Mn atoms with local moments oriented oppositely to the rest of the Mn moments [5, 7]. The value $c = 0$ describes the ferromagnetic (FM) state while the case $0 < c < x$ corresponds to a disordered local moment (DLM) state. The alloys with both substitutional and interstitial Mn atoms are described as $(Ga_{1-x+z}Mn_{x-z})AsMn^{i}_{z}$ where $x$ denotes the total content of Mn atoms while $z$ ($0 \leqslant z \leqslant x$) is the content of Mn interstitials. The latter were placed randomly in tetrahedral hollow sites surrounded by four anions [13] and two orientations of the interstitial Mn moments with respect to the substitutional Mn moments were considered: a FM state and an antiferromagnetic (AFM) state.

The self-consistent electronic structure calculations within the local spin-density approximation (LSDA) [14] were performed using the all-electron scalar-relativistic tight-binding linear muffin-tin orbital (TB-LMTO) method in the atomic-sphere approximation [15, 16]. We employ empty spheres in tetrahedral interstitial positions of the zinc-blende lattice to achieve a good space filling and use equal Wigner–Seitz radii for all atoms and empty spheres. The valence basis comprised s-, p-, and d-type orbitals, the local exchange–correlation potential was parametrized according to [17], the substitutional randomness as well as the DLM state were treated in the coherent potential approximation (CPA) [16, 18], and the Brillouin-zone (BZ) integrals were evaluated using 1638 **k**-points in the irreducible wedge of the fcc BZ.

The residual resistivity $\rho$ was evaluated using the Kubo–Greenwood linear response theory for substitutionally disordered systems as

$$\rho = \sigma^{-1}, \qquad \sigma = \sigma^{\mu\mu,\uparrow} + \sigma^{\mu\mu,\downarrow}, \tag{1}$$

where the conductivity $\sigma$ is equal to the sum over two spin channels $s$ ($s = \uparrow, \downarrow$) of diagonal elements $\sigma^{\mu\mu,s}$ ($\sigma^{xx,s} = \sigma^{yy,s} = \sigma^{zz,s}$) of the spin-dependent conductivity tensor $\sigma^{\mu\nu,s}$. We use a formulation for $\sigma^{\mu\nu,s}$ based on the intersite (interatomic) electron transport [19] which leads to

$$\sigma^{\mu\nu,s} = -\frac{e^2}{\pi\hbar V_0 N}\mathrm{Tr}\left\langle \mathrm{Im}\, g^s(E_\mathrm{F}^+) D^\mu \,\mathrm{Im}\, g^s(E_\mathrm{F}^+) D^\nu \right\rangle, \tag{2}$$

where $\mu, \nu = x, y, z$ are the Euclidean indices, $V_0$ is the volume of the primitive cell, $N$ is the number of cells in a large but finite solid with three-dimensional periodic boundary conditions, and $\langle\cdots\rangle$ denotes the configurational averaging. The trace in (2) extends over the site index $\mathbf{R}$ and the angular momentum index $L = (\ell, m)$, the quantities $g^s(z)$ and $D^\mu$ are matrices in the $\mathbf{R}L$-index, $\mathrm{Im}\, M = (M - M^+)/(2\mathrm{i})$ denotes the anti-Hermitian part of a matrix $M$, and $E_\mathrm{F}^+ = E_\mathrm{F} + \mathrm{i}0$ where $E_\mathrm{F}$ is the system Fermi energy. The matrix $g^s(z) = \{g^s_{\mathbf{R}L,\mathbf{R}'L'}(z)\}$ denotes the so-called auxiliary Green function while the matrix $D^\mu$ represents an effective velocity operator defined as

$$D^\mu = X^\mu S - S X^\mu, \tag{3}$$

where $S = \{S_{\mathbf{R}L,\mathbf{R}'L'}\}$ is the matrix of structure constants of the TB-LMTO method and $X^\mu$ is a position operator. The latter is expressed in a particularly simple manner, namely as

$$X^\mu_{\mathbf{R}L,\mathbf{R}'L'} = X^\mu_{\mathbf{R}}\delta_{\mathbf{R}L,\mathbf{R}'L'}, \tag{4}$$

where $X^\mu_{\mathbf{R}}$ denotes the $\mu$th component of the vector $\mathbf{R}$ [19]. The configurational average in (2) can be reduced to four averages of the form [18]

$$\mathrm{Tr}\left\langle g^s(z) D^\mu g^s(z') D^\nu \right\rangle = \mathrm{Tr}\left[\bar{g}^s(z) D^\mu \bar{g}^s(z') D^\nu\right] + \xi^{\mu\nu,s}(z, z'), \tag{5}$$

where the energy arguments $z, z'$ acquire two values $E_\mathrm{F}^+$ and $E_\mathrm{F}^- = E_\mathrm{F} - \mathrm{i}0$, and $\bar{g}^s(z) = \langle g^s(z)\rangle$ denotes the configurationally averaged Green-function matrix. The first term in (5) is the coherent part while the second term includes the corresponding vertex corrections. Since the velocity operators $D^\mu$ are non-random quantities, the vertex corrections can be formulated in a standard way [20]. The result is

$$\begin{aligned}\xi^{\mu\nu,s}(z, z') = \sum_{\mathbf{R}_1\Lambda_1}\sum_{\mathbf{R}_2\Lambda_2} &\left\{\bar{g}^s(z') D^\nu \bar{g}^s(z)\right\}_{\mathbf{R}_1 L_1', \mathbf{R}_1 L_1} \\ &\times \left\{[1 - w^s(z, z')\chi^s(z, z')]^{-1} w^s(z, z')\right\}_{\mathbf{R}_1\Lambda_1, \mathbf{R}_2\Lambda_2} \\ &\times \left\{\bar{g}^s(z) D^\mu \bar{g}^s(z')\right\}_{\mathbf{R}_2 L_2, \mathbf{R}_2 L_2'},\end{aligned} \tag{6}$$

where $\Lambda_1 = (L_1, L_1')$, $\Lambda_2 = (L_2, L_2')$ are composite indices and the matrix quantities $w^s(z, z')$ and $\chi^s(z, z')$ are defined as

$$\begin{aligned} w^s_{\mathbf{R}_1\Lambda_1,\mathbf{R}_2\Lambda_2}(z, z') &= \delta_{\mathbf{R}_1\mathbf{R}_2}\sum_Q c^Q_{\mathbf{R}_1} t^{Q,s}_{\mathbf{R}_1;L_1L_2}(z) t^{Q,s}_{\mathbf{R}_1;L_2'L_1'}(z'), \\ \chi^s_{\mathbf{R}_1\Lambda_1,\mathbf{R}_2\Lambda_2}(z, z') &= \left(1 - \delta_{\mathbf{R}_1\mathbf{R}_2}\right)\bar{g}^s_{\mathbf{R}_1L_1,\mathbf{R}_2L_2}(z)\bar{g}^s_{\mathbf{R}_2L_2',\mathbf{R}_1L_1'}(z'), \end{aligned} \tag{7}$$

where $Q$ runs over the atomic species occupying the lattice sites $\mathbf{R}$ with concentrations $c^Q_{\mathbf{R}}$ and $t^{Q,s}_{\mathbf{R};LL'}(z)$ denotes the single-site $t$-matrix resulting from embedding a single $Q$-impurity into the effective CPA medium [16]. As a consequence of the very simple form of the position

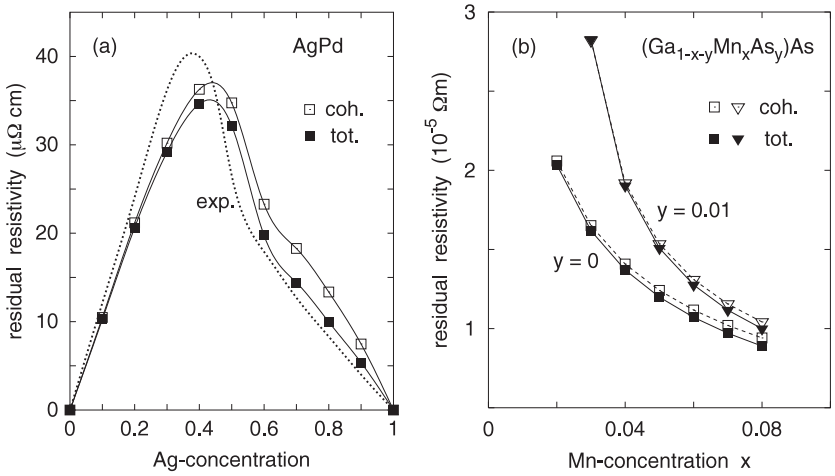


**Figure 1.** (a) The residual resistivity of disordered fcc Ag–Pd alloys calculated by the present TB-LMTO approach: from the coherent part of the conductivity (open squares) and from the total conductivity including the vertex corrections (full squares). The dotted curve denotes experimental results [21]. (b) The residual resistivity of the $(Ga_{1-x-y}Mn_xAs_y)As$ alloy as a function of the Mn content: without As antisites ($y = 0$, squares) and with 1% As antisites ($y = 0.01$, triangles). The open and full symbols relate to the coherent and the total conductivities, respectively.

operator (4), the on-site elements in (6) vanish identically for $z = z'$ ($\{\bar{g}^s(z)D^\mu \bar{g}^s(z)\}_{\mathbf{R}L,\mathbf{R}L'} = 0$), so $\xi^{\mu\nu,s}(z, z) = 0$ and the conductivity tensor (2) can be expressed as

$$\sigma^{\mu\nu,s} = -\frac{e^2}{\pi\hbar V_0 N}\left\{\mathrm{Tr}\left[\mathrm{Im}\,\bar{g}^s(E_\mathrm{F}^+)D^\mu\,\mathrm{Im}\,\bar{g}^s(E_\mathrm{F}^+)D^\nu\right] + \tfrac{1}{4}\left[\xi^{\mu\nu,s}(E_\mathrm{F}^+, E_\mathrm{F}^-) + \xi^{\mu\nu,s}(E_\mathrm{F}^-, E_\mathrm{F}^+)\right]\right\}. \tag{8}$$

Its evaluation employs the lattice Fourier transforms of all matrix quantities [19]. The corresponding BZ averages were calculated using $7 \times 10^6$ **k**-points in the full fcc BZ.

The scheme developed has been tested for random fcc AgPd alloys. The results for the coherent part of the conductivity (first term in (8)) have been discussed in detail in [19]; the role of the vertex corrections is shown in figure 1(a). It is seen that the vertex corrections are negligible for Pd-rich alloys while their effect for the Ag-rich alloys is about 30%, in excellent quantitative agreement with a previous study using the Korringa–Kohn–Rostoker method [22].

## 3. Results and discussion

### *3.1. Residual resistivities*

Since the electronic structure of the alloys studied (without Mn interstitials) has been discussed elsewhere [9], we will focus here on the residual resistivities. Their calculated values for a typical Mn content of 5% lie in the range $1–5 \times 10^{-5}\ \Omega$ m (see below), in good agreement with experiment [1, 12]. The dependence of $\rho$ on the Mn content $x$ for two different concentrations $y$ of As antisites is shown in figure 1(b). The vertex part of the conductivity is very small, similarly to the Pd-rich case for AgPd alloys. However, we observe a decrease of the resistivity with the concentration of Mn impurities, which is just the opposite dependence to that known for metallic alloys. The reason for such behaviour is a competition of two trends in the DMSs:

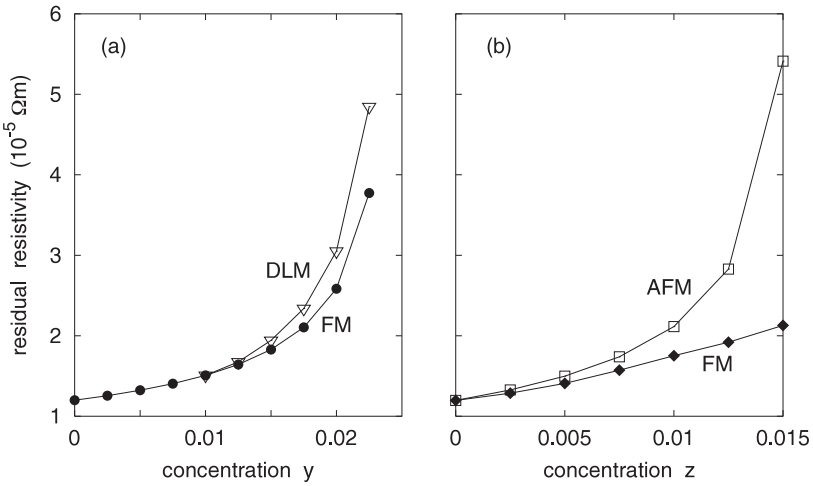


**Figure 2.** The residual resistivity of (Ga, Mn)As alloys with native structural defects: (a) as a function of the As antisite concentration $y$ in the $(Ga_{0.95-y}Mn_{0.05}As_y)As$ alloy for the ferromagnetic state (FM, full circles) and for a disordered local moment state (DLM, open triangles); (b) as a function of the Mn interstitial concentration $z$ in the $(Ga_{0.95+z}Mn_{0.05-z})AsMn^{i}_{z}$ alloy for the antiferromagnetic (AFM, open squares) and ferromagnetic (FM, full diamonds) alignment of magnetic moments on the substitutional and interstitial Mn atoms.

(i) the increase of $\rho$ with increasing concentration of defects which is due to impurity scatterings, and
(ii) the increase of the conductivity, i.e., the decrease of $\rho$, with increasing number of carriers which is in turn proportional to the concentration of Mn atoms.

The dependence on the number of carriers (valence holes) is particularly pronounced for Mn concentrations close to the compensated case, e.g., for $x \to 0.02$ at $y = 0.01$. Such a strong dependence on the number of carriers is lacking in typical metallic alloys with a large number of carriers at the Fermi energy only weakly depending on the alloy composition. It should be noted that for the case without As antisites we have a completely filled minority valence band (half-metallic behaviour), so $\sigma^{\downarrow} = 0$, and the current is carried only by majority electrons, $\rho = 1/\sigma^{\uparrow}$.

The effect of native compensating defects on $\rho$ for (Ga, Mn)As alloys with 5% Mn is summarized in figure 2. The resistivity monotonically increases with the As antisite content $y$ and it diverges in the fully compensated case ($y \to 0.025$); see figure 2(a). While this looks like a conventional metallic behaviour, the dominating effect is again the reduction of the number of carriers with increasing $y$. We have found that for $y > 0.0115$ the magnetic ground state is a DLM state rather than the FM state [7] (see also [5]). The resistivity of the FM state is smaller as compared to the DLM state because the magnetic disorder leads to an additional scattering resulting in an increased $\rho$ (the numbers of carriers are the same in the two cases).

The effect of Mn interstitials on $\rho$ is illustrated in figure 2(b) for both FM and AFM states; we have found that the AFM state has a lower energy than the FM state. The resistivity increases with the Mn interstitial content $z$ for both states; however, the two dependences differ from each other. In particular, the resistivity in the AFM case quickly increases if we approach the fully compensated state ($z \to 0.0166\ldots$). In contrast, the resistivity for the FM state increases with $z$ nearly linearly over the whole concentration range studied. One

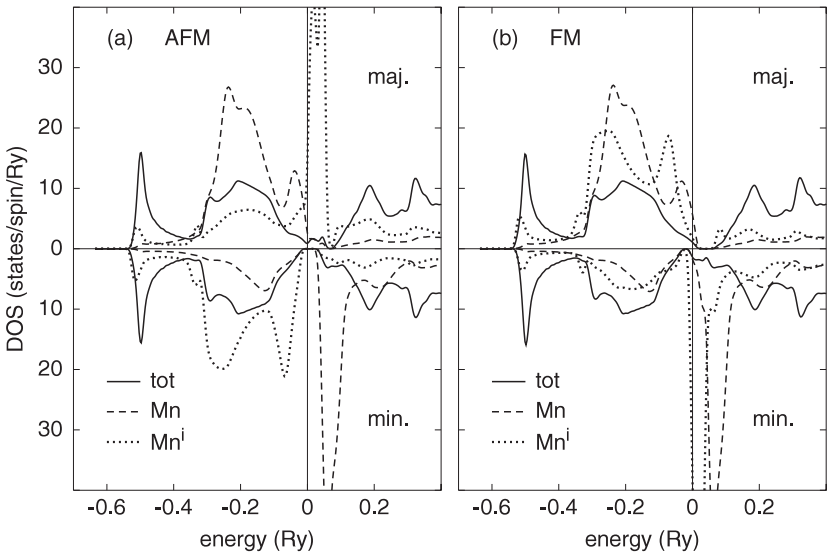


**Figure 3.** Spin-resolved total densities of states (full curves) and local Mn densities of states on substitutional (Mn, dashed curves) and interstitial ($Mn^i$, dotted curves) atoms for the $(Ga_{0.95+z}Mn_{0.05-z})AsMn^i_z$ alloy at the compensated composition ($z = 0.0166\ldots$) with antiferromagnetic (a) and ferromagnetic (b) alignment of the substitutional and interstitial Mn moments. The energy zero coincides with the Fermi level.

can understand such a difference from the corresponding densities of states shown in figure 3 for $z$ close to the compensation limit. The AFM state exhibits a conventional half-metallic behaviour with $E_F$ in the gap of the minority states, so the conductivity is due to the majority carriers only. The large resistivity is due to the Fermi level lying in the energy region of strongly disordered Mn interstitial states formed in the majority band gap; see figure 3(a). In contrast, $E_F$ for the FM case lies in the minority conduction band—see figure 3(b)—and both majority and minority carriers contribute to the conductivity, so the resistivity is smaller as compared to the AFM case. It should be noted that the densities of states for the FM state are in a good agreement with results of full-potential supercell calculations [13].

### *3.2. Correlation between conductivities and Curie temperatures*

The first-principles zero-temperature electronic structure calculations represent a suitable starting point for studying the exchange interactions between the local Mn moments in the framework of an effective classical Heisenberg Hamiltonian [7, 9]. The pair exchange interactions are obtained from a mapping of changes of total energy due to infinitesimal changes of direction of the local moments. In the present study, we have employed the derived pair interactions in a simple quantitative estimation of the Curie temperatures using a mean-field approximation; see [7, 9] for details. Figure 4 shows the experimentally observed correlation between the conductivity (measured at 4.2 K) and the Curie temperature for thin (Ga, Mn)As films with 5% Mn, and the theoretical correlation calculated for $(Ga_{0.95-y}Mn_{0.05}As_y)As$ alloys ($0 \leqslant y < 0.025$) with the DLM ground state for $y > 0.0115$. Considering the different systems in the experiment (thin films) and the calculations (bulk alloys), the semiquantitative agreement obtained is quite satisfactory. These results witness that both quantities reflect mainly the degree of compensation (number of holes) in the DMSs studied.

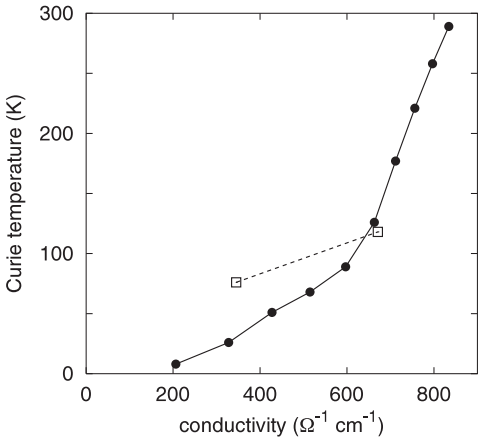


**Figure 4.** The Curie temperatures versus the residual conductivities as calculated for $(Ga_{0.95-y}Mn_{0.05}As_y)As$ alloys with varying As antisite content $y$ (full dots) and the experimental values obtained for as-grown and annealed $Ga_{0.95}Mn_{0.05}As$ thin films [12] (open squares).

## 4. Conclusions

The main results of our systematic LSDA-CPA study of the residual resistivity of p-type (Ga, Mn)As alloys can be summarized as follows:

(i) the order of magnitude of the calculated resistivities agrees reasonably well with experimental data;
(ii) the concentration trends of the resistivity reflect the strength of the impurity scattering and the number of carriers (holes in the valence band);
(iii) the resistivity decreases as a function of the Mn concentration but it increases with increasing content of native compensating defects (As antisites, Mn interstitials);
(iv) the resistivity of the ferromagnetic state is smaller than that of more complicated spin arrangements (disordered local moments, antiferromagnetic state);
(v) the conductivities and the Curie temperatures are strongly correlated, in agreement with experiment;
(vi) the vertex corrections to the conductivity are weak in the systems studied.

## Acknowledgments

The authors acknowledge the financial support provided by the Czech Science Foundation (202/04/0583), the Academy of Sciences of the Czech Republic (A1010203, S2041105), the CMS Vienna (GZ 45.504), and the RT Network 'Computational Magnetoelectronics' (Contract HPRN-CT-2000-00143) of the European Commission.

## References

[1] Ohno H 1999 *J. Magn. Magn. Mater.* **200** 110
[2] Dietl T, Ohno H, Matsukura F, Cibert J and Ferrand D 2000 *Science* **287** 1019
[3] Park Y D *et al* 2002 *Science* **295** 651
[4] Akai H 1998 *Phys. Rev. Lett.* **81** 3002
[5] Korzhavyi P A *et al* 2002 *Phys. Rev. Lett.* **88** 187202

[6] Sandratskii L M and Bruno P 2002 *Phys. Rev.* B **66** 134435
[7] Kudrnovský J, Turek I, Drchal V, Máca F, Mašek J, Weinberger P and Bruno P 2003 *J. Supercond.* **16** 119
[8] Sato K, Dederichs P H and Katayama-Yoshida H 2003 *Europhys. Lett.* **61** 403
[9] Kudrnovský J, Turek I, Drchal V, Máca F, Weinberger P and Bruno P 2004 *Phys. Rev.* B **69** 115208
[10] Jungwirth T, Niu Q and MacDonald A H 2002 *Phys. Rev. Lett.* **88** 207208
[11] Jungwirth T, Abolfath M, Sinova J, Kučera J and MacDonald A H 2002 *Appl. Phys. Lett.* **81** 4029
[12] Edmonds K W *et al* 2002 *Appl. Phys. Lett.* **81** 4991
[13] Máca F and Mašek J 2002 *Phys. Rev.* B **65** 235209
[14] von Barth U and Hedin L 1972 *J. Phys. C: Solid State Phys.* **5** 1629
[15] Andersen O K and Jepsen O 1984 *Phys. Rev. Lett.* **53** 2571
[16] Turek I, Drchal V, Kudrnovský J, Šob M and Weinberger P 1997 *Electronic Structure of Disordered Alloys, Surfaces and Interfaces* (Boston, MA: Kluwer)
[17] Vosko S H, Wilk L and Nusair M 1980 *Can. J. Phys.* **58** 1200
[18] Weinberger P 1990 *Electron Scattering Theory for Ordered and Disordered Matter* (Oxford: Clarendon)
[19] Turek I, Kudrnovský J, Drchal V, Szunyogh L and Weinberger P 2002 *Phys. Rev.* B **65** 125101
[20] Velický B 1969 *Phys. Rev.* **184** 614
[21] Coles B R and Taylor J C 1962 *Proc. R. Soc.* A **267** 139
[22] Swihart J C, Butler W H, Stocks G M, Nicholson D M and Ward R C 1986 *Phys. Rev. Lett.* **57** 1181